

---

# AutoST : Training-free Neural Architecture Search for Spiking Transformers

---

**Ziqing Wang<sup>1</sup>, Qidong Zhao<sup>1</sup>, Jinku Cui<sup>1</sup>, Xu Liu<sup>1</sup>, Dongkuan Xu<sup>1\*</sup>**

<sup>1</sup> North Carolina State University

## Abstract

Spiking Transformers have gained considerable attention because they achieve both the energy efficiency of Spiking Neural Networks (SNNs) and the high capacity of Transformers. However, the existing Spiking Transformer architectures, derived from ANNs, exhibit a notable architectural gap, resulting in suboptimal performance compared to their ANN counterparts. Traditional approaches to discovering optimal architectures primarily rely on either manual procedures, which are time-consuming, or Neural Architecture Search (NAS) methods, which are usually expensive in terms of memory footprints and computation time. To address these limitations, we introduce AutoST, a training-free NAS method for Spiking Transformers, to rapidly identify high-performance and energy-efficient Spiking Transformer architectures. Unlike existing training-free NAS methods, which struggle with the non-differentiability and high sparsity inherent in SNNs, we propose to utilize Floating-Point Operations (FLOPs) as a performance metric, which is independent of model computations and training dynamics, leading to a stronger correlation with performance. Moreover, to enable the search for energy-efficient architectures, we leverage activation patterns during initialization to estimate the energy consumption of Spiking Transformers. Our extensive experiments show that AutoST models outperform state-of-the-art manually or automatically designed SNN architectures on static and neuromorphic datasets, while significantly reducing energy consumption.

## 1 Introduction

Spiking neural networks (SNNs) have gained extensive attention as brain-inspired computational models, owing to their remarkable energy efficiency and ability to emulate the spiking behavior of biological neurons [25]. Concurrently, the Transformer architecture, originally developed for natural language processing, has exhibited impressive performance in a wide array of computer vision tasks [36; 13; 24]. This has led to a growing interest in integrating SNNs with Transformers to develop Spiking Transformers, which makes it possible to achieve high energy efficiency and superior performance. Recent advancements reveal successful applications of Spiking Transformers across multiple domains, such as classification [38], tracking [43; 30], and recognition tasks [17].

Despite these successes, existing Spiking Transformer architectures predominantly rely on ANN-based architectures. This dependence tends to overlook the unique properties of SNNs, resulting in less optimal performance compared to their ANN counterparts [20; 31]. As illustrated in Fig. 1, there is a substantial variation in accuracy and energy consumption across different SNN architectures. This variation highlights the need for a more in-depth investigation of the design choices involved in the development of Spiking Transformer architectures. Finding optimal SNN architectures has traditionally been pursued via two common approaches. The first involves manually designing architectures, which is a labor-intensive endeavor [20] and does not guarantee optimal results [47].

---

\*Corresponding author

The second approach involves utilizing Neural Architecture Search (NAS) methods to automatically discover the ideal architecture. However, most existing NAS methods require multiple training stages or a single supernet training that encompasses all architecture candidates [3; 4; 8], leading to longer convergence times compared to standard training. Considering that the SNNs generally exhibit slower training speeds compared to their ANN counterparts, the application of these NAS methods to SNNs is challenging [20]. Furthermore, Transformer models have considerably larger search spaces than CNNs and require more training epochs [47], rendering these NAS methods insufficient.

To address these limitations, we propose, for the first time, to leverage training-free NAS to rapidly identify high-performance and energy-efficient Spiking Transformer architectures. Recent training-free NAS approaches [47; 26; 1; 23; 10], which search for the optimal architecture from initialized networks without any training, substantially reduce search times. Nevertheless, it is not straightforward to directly apply these existing training-free NAS methods to Spiking Transformers. Most current methods, developed for ANNs, rely on gradients during a backward pass; however, the spike is non-differentiable during backpropagation in SNNs, leading to inaccurate gradients. Moreover, methods employing activation patterns introduce significant errors due to the inherent high sparsity of SNNs [20].

In this work, we propose `AutoST`, a training-free NAS to search for superior Spiking Transformer architectures. The main contributions of our work are as follows:

- We propose to utilize Floating-Point Operations (FLOPs) as a performance metric, which is independent of model computations and training dynamics, thus effectively tackling the challenges posed by non-differentiability and high sparsity inherent to SNNs, leading to a stronger correlation with performance. To the best of our knowledge, `AutoST` is the first implementation of NAS to explore Spiking Transformer architectures.
- Extensive experiments show that our searched `AutoST` models outperform state-of-the-art SNNs on both static and neuromorphic datasets. In particular, the accuracy of our `AutoST` model outperforms that of the SNN models searched by other NAS methods by 3.06%, 4.34%, and 9.47% on the CIFAR-10, CIFAR-100, and Tiny-ImageNet datasets, respectively.
- To achieve a balance between performance and energy efficiency, we leverage activation patterns to estimate the energy consumption of Spiking Transformer architectures during initialization. In specific, our `AutoST` model achieves a 1.3% improvement in accuracy while reducing energy consumption by 53.9% on the CIFAR-100 dataset compared to other state-of-the-art Spiking Transformer architectures.

## 2 Related Work

**Spiking Neural Networks.** SNNs have garnered significant attention in the field of brain-inspired intelligence due to their compatibility with neuromorphic hardware and biological properties [9; 39]. With the growing interest in larger-scale and higher-performance SNNs, recent research has concentrated on developing innovative training algorithms and architectures. tdBn [45] proposed a threshold-dependent batch normalization based on spatiotemporal backpropagation. Additionally, [45; 34; 14] proposed novel architectures for residual learning in deep SNNs to overcome the gradient vanishing problem. However, the performance of these methods has yet to match their ANN counterparts, which limits the application of SNNs. Consequently, our work aims to search for superior SNN architectures that can narrow the performance gap between SNNs and ANNs.

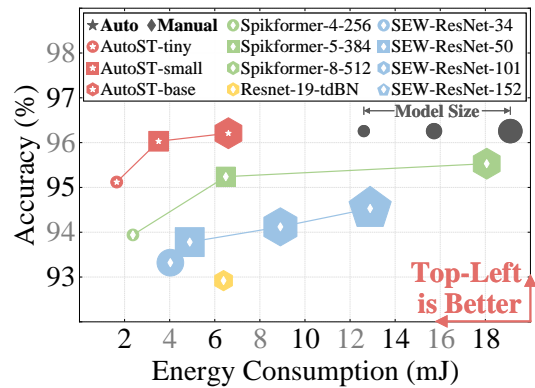


Figure 1: Comparison between `AutoST` and state-of-the-art SNN models of accuracy and energy consumption on the CIFAR-10 dataset. The models located in the top-left quadrant represent superior performance (higher accuracy and lower energy consumption). The marker sizes represent the relative model sizes. Star-shaped and diamond-shaped hollows within the markers denote manually and automatically designed models, respectively.

To address these limitations, we propose, for the first time, to leverage training-free NAS to rapidly identify high-performance and energy-efficient Spiking Transformer architectures. Recent training-free NAS approaches [47; 26; 1; 23; 10], which search for the optimal architecture from initialized networks without any training, substantially reduce search times. Nevertheless, it is not straightforward to directly apply these existing training-free NAS methods to Spiking Transformers. Most current methods, developed for ANNs, rely on gradients during a backward pass; however, the spike is non-differentiable during backpropagation in SNNs, leading to inaccurate gradients. Moreover, methods employing activation patterns introduce significant errors due to the inherent high sparsity of SNNs [20].

In this work, we propose `AutoST`, a training-free NAS to search for superior Spiking Transformer architectures. The main contributions of our work are as follows:

- We propose to utilize Floating-Point Operations (FLOPs) as a performance metric, which is independent of model computations and training dynamics, thus effectively tackling the challenges posed by non-differentiability and high sparsity inherent to SNNs, leading to a stronger correlation with performance. To the best of our knowledge, `AutoST` is the first implementation of NAS to explore Spiking Transformer architectures.
- Extensive experiments show that our searched `AutoST` models outperform state-of-the-art SNNs on both static and neuromorphic datasets. In particular, the accuracy of our `AutoST` model outperforms that of the SNN models searched by other NAS methods by 3.06%, 4.34%, and 9.47% on the CIFAR-10, CIFAR-100, and Tiny-ImageNet datasets, respectively.
- To achieve a balance between performance and energy efficiency, we leverage activation patterns to estimate the energy consumption of Spiking Transformer architectures during initialization. In specific, our `AutoST` model achieves a 1.3% improvement in accuracy while reducing energy consumption by 53.9% on the CIFAR-100 dataset compared to other state-of-the-art Spiking Transformer architectures.

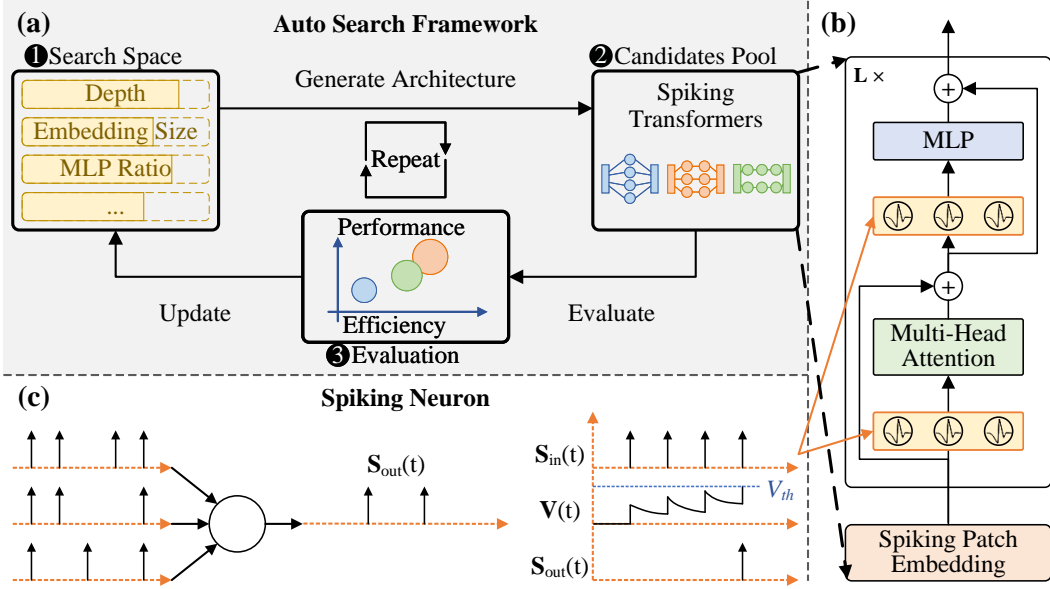


Figure 2: Overview of AutoST. Subfigure (a) shows the AutoST pipeline: ① Initial generation of architecture candidates within a predefined search space; ② Selection of Spiking Transformer architectures from the candidate pool; ③ Evaluation of selected architectures based on proposed training-free metrics for performance and efficiency. Subfigure (b) presents the overall architecture of Spiking Transformers. Subfigure (c) illustrates the operation of a spiking neuron, which transmits spikes to the subsequent layer when the membrane potential  $V(t)$  surpasses the threshold  $V_{th}$ .

**Spiking Transformers.** The integration of Transformers and SNNs has the potential to achieve enhanced performance while reducing power consumption. STNet [43] and Spike-T [44] employed separate branches of SNNs and Transformers for feature extraction. However, such approaches limit the ability to run independently on neuromorphic hardware and fail to fully exploit the energy efficiency benefits of SNNs. Furthermore, Mueller et al. [30] proposed a Spiking Transformer using the ANN-to-SNN conversion method, but their design did not incorporate the self-attention module within SNNs. The recently proposed Spikformer [48] directly trained the Transformer in SNNs, yet it still struggles to achieve performance comparable to leading ANNs. In light of these limitations, our work aims to search for superior Spiking Transformer architectures to exploit the full potential of SNNs and Transformers, thereby improving their performance and energy efficiency.

**Neural Architecture Search.** Early NAS algorithms employed reinforcement learning [49; 50] or evolutionary algorithms [33]. However, these methods are computationally expensive. To mitigate this issue, weight-sharing approaches have been introduced [3; 4; 8], which eliminate the need for training the architecture from scratch at each search step, resulting in improved efficiency compared to previous NAS methods. Recently, training-free NAS methods [10; 2; 27] do not require training during the search stage, significantly reducing the computational cost associated with identifying optimal architectures. Despite the considerable progress made by NAS methods in the ANN domain, NAS for Spiking Transformers has yet to be developed. In this work, we aim to construct superior Spiking Transformer architectures by leveraging NAS technique.

### 3 Preliminary

#### 3.1 Spiking Neuron Model

Unlike traditional ANNs, SNNs utilize binary spike trains to convey information. As shown in Fig. 2, we employ the widely adopted Leaky-Integrate-and-Fire (LIF) model to mimic the dynamics of spiking neurons. The LIF model is defined as follows:

$$H[t] = V[t-1] + \frac{1}{\tau} (X[t] - (V[t-1] - V_{reset})), \quad (1)$$

$$S[t] = \Theta(H[t] - V_{th}), \quad (2)$$

$$V[t] = H[t](1 - S[t]) + V_{reset} S[t], \quad (3)$$

where  $\tau$  denotes the membrane time constant,  $X[t]$  represents the input current at the timestep  $t$ . When the membrane potential  $V[t]$  exceeds the firing threshold  $V_{th}$  at the timestep  $t$ , a spike  $S[t]$

will be generated by the spiking neuron to the next layer. The Heaviside step function  $\Theta(v)$  equals 1 for  $v \geq 0$  and 0 otherwise.  $V[t]$  represents the membrane potential post the triggering event, which equals  $H[t]$  if no spike is produced and is otherwise reset to the potential  $V_{\text{reset}}$ .

### 3.2 Training-free Neural Architecture Search

Training-free NAS evaluates model performance without actual training, thus largely reducing the search time. Existing methods often rely on the sum of weight saliency values as a performance metric [47; 2; 21; 37]. Other studies focus on the properties of architectural representation, such as expressivity [23; 10; 27]. Mellor et al. [27] propose the use of linear regions, where the activation patterns of linear regions are used for measuring the discriminative ability of a model.

## 4 Training-free NAS for Spiking Transformers

### 4.1 Performance Prediction via FLOPs

In this section, we first explore the application of recent training-free metrics for NAS in the context of Spiking Transformers. Many existing metrics require forward and backward passes through the architecture to compute a score, such as SynFlow [35], Snip [21] and NTK [19].

However, SNNs undergo a Heaviside step function during forward propagation, leading to non-differentiability during backward propagation. This intrinsic characteristic of SNNs can result in inaccurate gradient calculations and potentially unreliable metric scores. Furthermore, while the LinearRegions method [27] circumvents the need for a backward pass, it faces challenges due to large variations in the sparsity of activation patterns in SNNs [20]. These variations in sparsity impact the suitability of the LinearRegions method for Spiking Transformers. To overcome these constraints, we propose the use of FLOPs as a metric to predict the final performance of the model. This approach is solely related to the self-characterization of the model and eliminates the need for forward/backward propagation, effectively circumventing both the non-differentiability and sparsity variation issues.

The computation of FLOPs in a Transformer model is predominantly attributed to two components: the Self Attention (SA) block and the Multi-layer Perceptron (MLP) block. We present the computation for each component as follows:

$$\text{FLOPs}_{\text{SA}} = L \times n \times d_{\text{model}} \times (2d_{\text{model}} + n) \quad (4)$$

$$\text{FLOPs}_{\text{MLP}} = L \times n \times (d_{\text{model}} \times d_{\text{mlp}} + d_{\text{mlp}} \times d_{\text{model}}) \quad (5)$$

For the SA block,  $\text{FLOPs}_{\text{SA}}$  denotes the total number of floating-point operations required, where  $L$  represents the number of layers,  $n$  the sequence length, and  $d_{\text{model}}$  is the embedding dimension of the model. For the MLP block,  $d_{\text{mlp}}$  represents the hidden dimension.

The computation of the FLOPs of Spiking Transformers is similar to the process for ANN Transformers, with additional consideration for the time dimension. To account for this, we multiply the FLOPs of the ANN-equivalent architecture by the number of timesteps:  $\text{FLOPs}_{\text{SNN}} = T \times \text{FLOPs}_{\text{ANN}}$ .

To demonstrate the effectiveness of our proposed metric, `AutoST`, we randomly sample 100 architectures from the small search space outlined in Tab. 2. We initially train these architectures for 100 epochs, compute the training-free metric scores, and then analyze their correlation with the final model performance. As shown in Tab. 1 and Fig. 3, our `AutoST` has high absolute values for both Kendall and Spearman coefficients. This suggests that the FLOPs metric has a strong correlation with model performance. This correlation is largely due to two factors. First, the FLOPs metric is independent of gradients, which allows it to circumvent the inherent non-differentiability of SNNs. Second, previous works assessed their metrics over a large parameter range, whereas, real-world applications often demand the identification of the optimal model within specific constraints (e.g., 4-4.5 M). In such circumstances, traditional metrics struggle to distinguish model

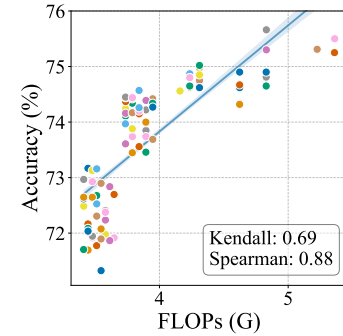


Figure 3: Performance Metric Evaluation: Evidence of a significant positive correlation between FLOPs and accuracy.

Table 1: Comparison of Correlation Coefficients: Analysis of the proposed metric against different training-free metrics. Note that absolute values of Kendall and Spearman coefficients approaching one indicate a stronger correlation between two variables. The search time represents the duration required to search 200 samples on the CIFAR-100 dataset with a single GPU. Our metric exhibits a pronounced correlation with the final accuracy and requires less time for searching.

Datasets	CIFAR-10		CIFAR-100		Tiny-ImageNet		Search Time (GPU Hours)
Metric	Kendall	Spearman	Kendall	Spearman	Kendall	Spearman	
NTK [19]	-0.43	-0.49	-0.40	-0.55	-0.49	-0.66	1.3
Snyflow [35]	0.57	0.77	0.56	0.76	0.56	0.75	0.6
LinearRegions [27]	0.58	0.85	0.59	0.79	0.60	0.81	0.2
SAHD [20]	0.56	0.81	0.52	0.74	0.49	0.67	0.2
<b>AutoST (ours)</b>	<b>0.70</b>	<b>0.91</b>	<b>0.69</b>	<b>0.88</b>	<b>0.62</b>	<b>0.86</b>	<b>0.2</b>

differences in such a narrow parameter range. In contrast, AutoST using FLOPs can effectively distinguish different models due to its calculation based on layer numbers and embedding dimensions. Moreover, since our method does not require a backward pass, it requires a shorter search time.

## 4.2 Energy Efficiency Estimation using Activation Patterns

The study of the energy efficiency of Spiking Transformer architectures has been somewhat overlooked. In this section, we propose a method to estimate the power consumption of Spiking Transformers during initialization. We initially compute the synaptic operations (SOPs) to determine the theoretical power consumption of Spiking Transformers:

$$\text{SOPs}(l) = fr \times T \times \text{FLOPs}(l) \quad (6)$$

where  $l$  represents a layer in the Transformer,  $fr$  is the firing rate of the input spike train of each layer, and  $T$  denotes the simulation timestep of the spiking neuron. FLOPs( $l$ ) refers to the floating-point operations of  $l$ , equivalent to the number of multiply-and-accumulate (MAC) operations, while SOPs account for the number of spike-based accumulate (AC) operations. Assuming that the MAC and AC operations are implemented on 45nm hardware, where  $E_{MAC} = 4.6pJ$  and  $E_{AC} = 0.9pJ$ , we calculate the theoretical power consumption of the Spiking Transformer based on [48; 18; 41]. The details of the computation of power consumption are shown in the Appendix.

However, calculating the theoretical power consumption typically requires the weights after training, which is not applicable in the context of training-free NAS. To address this issue, we propose using activation patterns as a proxy to estimate power consumption during initialization, following the approach proposed by [20; 27]. In a Rectified Linear Unit (ReLU) network, training samples partition tensors into active (positive values) and inactive (negative values) regions, forming binary masks. In the SNNs, these masks represent the spikes transmitted in the network, and their frequency directly affects power consumption. Spiking neurons with higher firing rates will consume more power due to the increased number of spike-based operations. Nevertheless, due to high sparsity variation in the temporal patterns of SNNs across different mini-batches, the measure of the distance of different activation patterns can be inaccurate. We address this issue by normalizing the distance measure based on the sparsity of the given activation patterns, similar to the method proposed in [20]. By analyzing the activation patterns and their Hamming distances, we can gain insight into the power consumption of the model and optimize Spiking Transformer architectures for improved efficiency.

As illustrated in Fig. 4, the activation pattern scores exhibit a strong relationship with power consumption. Consequently, the inverse of the activation pattern score can serve as an effective tool for evaluating the efficiency of Spiking Transformers in a training-free NAS setting.

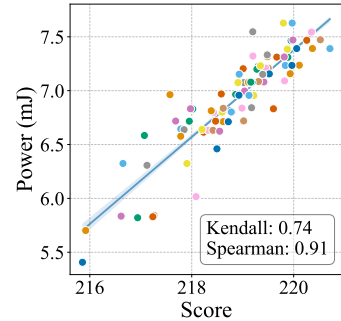


Figure 4: Efficiency Metric Evaluation: Demonstration of the strong positive correlation between activation scores and power consumption.

### 4.3 Balancing Performance and Efficiency

In the previous sections, we establish training-free metrics for both the performance and the efficiency of Spiking Transformers. In this section, we introduce the final `AutoST` score, which harmonizes these two aspects, thus capturing the trade-off between performance and efficiency. The final score of `AutoST` is defined as:

$$\text{Score}_{\text{AutoST}} = \text{Performance} + \lambda * \text{Efficiency} \quad (7)$$

where Performance is evaluated by the FLOPs, Efficiency is evaluated by the inverse of the activation patterns score.  $\lambda$  is a coefficient that modulates the contribution of the efficiency term. In practical applications,  $\lambda$  can be adjusted to optimize the trade-off between performance and efficiency to meet specific needs. This flexibility ensures that the model can adapt to a variety of scenarios, ranging from those demanding high computational performance to those where energy efficiency is paramount.

### 4.4 Overall Architecture of `AutoST`

The overall architecture of `AutoST` is based on [48], a purely transformer-based SNN. The overview of `AutoST` is depicted in Fig. 2. Considering an input 2D image sequence  $I \in \mathbb{R}^{T \times C \times H \times W}$ , a Spiking Patch Embedding (SPE) block is utilized for downsampling and partitioning the input into spiking patches  $X \in \mathbb{R}^{T \times N \times D}$ . These patches are subsequently passed through  $L$  Spiking Transformer Blocks, each comprising a Spiking Self Attention (SSA) block and a Spiking MLP (SMLP) block. The final stage consists of a Global Average Pooling (GAP) and a Fully Connected Layer (FC) serving as the classification head, outputting the prediction  $Y$ . The sequence of operations is mathematically defined as follows:

$$X = \text{SPE}(I), \quad I \in \mathbb{R}^{T \times C \times H \times W}, \quad X \in \mathbb{R}^{T \times N \times D} \quad (8)$$

$$X'_l = \text{SSA}(X_{l-1}) + X_{l-1}, \quad X'_l \in \mathbb{R}^{T \times N \times D}, \quad l = 1 \dots L \quad (9)$$

$$X_l = \text{SMLP}(X'_l) + X'_l, \quad X_l \in \mathbb{R}^{T \times N \times D}, \quad l = 1 \dots L \quad (10)$$

$$Y = \text{FC}(\text{GAP}(X_L)) \quad (11)$$

### 4.5 Search Space of `AutoST` under Different Resource Constraints

We design an extensive search space for `AutoST`, comprising four key variables in the Transformer: embedding size, number of heads, MLP ratio, and network depth, as detailed in Tab. 2. Based on these five variables, we design three distinct search spaces (Tiny, Small, and Base) for `AutoST`. Given the constraints on the model parameters, we divide the large-scale search space into three parts, as described in Tab. 2. This partitioning enables the search algorithm to focus on discovering models within a specific parameter range, allowing users to tailor their selections according to available resources and application needs.

Table 2: The search space of `AutoST`. Tuples in parentheses represent the lowest, highest value, and steps.

	<code>AutoST</code> -tiny	<code>AutoST</code> -small	<code>AutoST</code> -base
<b>Embed Size</b>	(192, 384, 64)	(256, 512, 64)	(384, 768, 64)
<b>MLP Ratio</b>	(3, 5, 1)	(3, 5, 1)	(3, 6, 1)
<b>Head Num</b>	(4, 8, 4)	(4, 8, 4)	(4, 8, 4)
<b>Depth</b>	(1,8,1)	(2,12,1)	(4,15,1)
<b># Params</b>	4-4.5M	11-12M	25-30M

### 4.6 Evolutionary Search Algorithm for Optimal `AutoST` under Resource Constraints

**Dual-Objective Evolutionary Search Strategy.** We conduct an evolutionary search to obtain the optimal `AutoST` under specified resource constraints. Our objective is dual-fold: maximizing classification accuracy and minimizing power consumption. At the start of the evolutionary search process, we randomly select  $N$  Spiking Transformer architectures that serve as the seed population. From these seeds, the top  $k$  performing architectures are selected as parent models to generate offspring for the next generation, utilizing crossover and mutation mechanisms. In each generation, the crossover mechanism selects two random parent candidates and merges their features to create new offspring. The mutation mechanism operates on two levels: firstly, the architecture's depth may mutate with a probability of  $P_d$ . Secondly, each individual block within the architecture has a chance to mutate with a probability of  $P_m$ , resulting in a newly configured architecture.

Table 3: Performance comparison between the proposed AutoST model and the state-of-the-art models on three different static datasets. \* represent the result of our implementation.

Dataset	Models	# Param (M)	Timesteps	Accuracy (%)	Model Type	Design Type
CIFAR-10	Spikformer-4-256 [48]	4.15	4	93.94	Transformer	Manual
	AutoSNN [29]	5.44	8	92.54	CNN	Auto
	SNASNet-Bw [5]	-	5	93.64	CNN	Auto
	AutoST -tiny (ours)	4.20	4	<b>95.14</b>	Transformer	Auto
	TET [11]	12.60	6	94.50	CNN	Manual
	DSR [28]	11.20	20	95.40	CNN	Manual
	Spikformer-5-384* [48]	11.32	4	95.24	Transformer	Manual
	SpikeDHS [29]	12.00	6	94.34	CNN	Auto
	AutoST -small (ours)	11.52	4	<b>96.03</b>	Transformer	Auto
	Diet-SNN [32]	39.90	5	93.44	CNN	Manual
CIFAR-100	RMP [16]	39.90	2048	93.63	CNN	Manual
	Spikformer-8-512* [48]	29.68	4	95.53	Transformer	Manual
	AutoSNN [29]	21.00	8	93.15	CNN	Auto
	AutoST -base (ours)	29.64	4	<b>96.21</b>	Transformer	Auto
	Spikformer-4-256 [48]	4.15	4	75.96	Transformer	Manual
	SNASNet-Bw [5]	-	5	73.04	CNN	Auto
	AutoSNN [29]	5.44	8	69.16	CNN	Auto
	AutoST -tiny (ours)	4.20	4	<b>76.29</b>	Transformer	Auto
	TET [11]	12.60	6	74.72	CNN	Manual
	DSR [28]	11.20	20	78.20	CNN	Manual
Tiny-ImageNet	Spikformer-5-384* [48]	11.32	4	78.12	Transformer	Manual
	SpikeDHS [5]	12.00	6	75.70	CNN	Auto
	AutoST -small (ours)	11.52	4	<b>79.44</b>	Transformer	Auto
	Diet-SNN [32]	39.90	5	69.67	CNN	Manual
	RMP [16]	39.90	2048	70.93	CNN	Manual
	Spikformer-8-512* [48]	29.68	4	78.48	Transformer	Manual
	AutoST -base (ours)	29.64	4	<b>79.69</b>	Transformer	Auto
	Spikformer-4-256* [48]	4.15	4	59.26	Transformer	Manual
	AutoSNN [29]	5.44	8	46.79	CNN	Auto
	AutoST -tiny (ours)	4.48	4	<b>59.78</b>	Transformer	Auto
Spikformer-5-384* [48]	Spikformer-5-384* [48]	11.32	4	61.98	Transformer	Manual
	SNASNet-Bw [5]	-	5	54.60	CNN	Auto
	AutoST -small (ours)	11.52	4	<b>63.07</b>	Transformer	Auto
	SPIKE-NORM [32]	38.38	5	54.20	CNN	Manual
	Spike-Thrift [16]	41.94	2048	51.92	CNN	Manual
	Dct-SNN [16]	36.87	2048	52.43	CNN	Manual
Spikformer-8-512* [48]	Spikformer-8-512* [48]	29.68	4	65.41	Transformer	Manual
	AutoST -base (ours)	29.87	4	<b>66.77</b>	Transformer	Auto

## 5 Experiments

### 5.1 Performance on Static Datasets

Tab. 3 provides a comprehensive performance comparison of our proposed model, AutoST, compared to existing state-of-the-art SNN models across CIFAR-10, CIFAR-100, and Tiny ImageNet datasets. We leverage three search spaces (Tiny, Small, Base) and select analogous SNN models for comparison. The results reveal that AutoST surpasses other SNN models in terms of top-1 accuracy.

**Tiny Models.** AutoST surpasses both Spikformer [48] and AutoSNN [29]. Specifically, the proposed AutoST surpasses AutoSNN, which is obtained through NAS, by 2.6%, 10.1%, and 13.01% on three datasets with fewer parameters and timesteps. This indicates that our model leverages the efficient search space of the AutoST, allowing for enhanced performance with reduced

model complexity. **Small Models.** The larger search space provides additional flexibility, potentially enhancing performance. Our `AutoST` outperforms Spikformer [48] in the same parameter range and yields higher accuracy compared to CNN-based models. Remarkably, `AutoST` not only outperforms the current state-of-the-art SNN model, DSR [28], in terms of accuracy but also demonstrates significantly fewer time steps, leading to lower SNN latency. This performance suggests that our `AutoST` method of utilizing an expanded search space can lead to significant performance gains in SNN architectures. **Base Models.** `AutoST` maintains its superior performance, outperforming all other models with substantially fewer parameters in a larger search space. This further highlights the effectiveness and efficiency of our proposed method, potentially opening new avenues for SNN research.

## 5.2 Performance on Neuromorphic Datasets

We further demonstrate the superiority of the `AutoST` method by evaluating its performance on neuromorphic datasets. We compare our model with state-of-the-art SNN models on the CIFAR10-DVS dataset. Due to the overfitting issue on neuromorphic datasets, we restrict our comparison to the tiny model. Tab. 4 reveals that the `AutoST` model achieves the highest top-1 accuracy, outperforming the existing state-of-the-art SNN models. Notably, `AutoST` outperforms SEW-ResNet [46] by 7.2% while maintaining far fewer parameters. These results further validate the effectiveness of our proposed method and its strong generalization capabilities when applied to neuromorphic datasets.

Table 4: Performance comparison on the CIFAR10-DVS dataset. **Ts** stands for the timesteps of SNNs.

Methods	Ts	Acc (%)	Model	Design
<b>tdBN</b> [46]	10	67.8	CNN	Manual
<b>LIAF-Net</b> [40]	10	70.4	CNN	Manual
<b>PLIF</b> [15]	20	74.8	CNN	Manual
<b>Dspkie</b> [22]	10	75.4	CNN	Manual
<b>DSR</b> [28]	10	77.3	CNN	Manual
<b>SEW-ResNet</b> [46]	16	74.4	CNN	Manual
<b>Spikformer</b> [48]	16	80.9	Transformer	Manual
<b>AutoSNN</b> [29]	8	72.5	CNN	Auto
<b>AutoST (ours)</b>	16	<b>81.6</b>	Transformer	Auto

## 5.3 Performance and Energy-efficiency Trade-off

In our previous experiments, the coefficient  $\lambda$  in Equation 7 is set to zero, indicating that only the performance metric is considered. In this section, we delve deeper and explore optimal Spiking Transformer architectures under a spectrum of  $\lambda$  values.  $\lambda$  is calibrated based on the scale of performance and efficiency measures. As shown in Tab. 5, incrementally augmenting the value of  $\lambda$  bolsters the impact of the efficiency term. However, beyond a certain threshold, increasing  $\lambda$  consistently produces the same architectures, suggesting that an optimal point of energy efficiency has been reached under the model constraints. Remarkably, the proposed `AutoST` model attains only 56.7% of the power consumption of its ANN counterparts, with a negligible accuracy trade-off of 0.87%. In comparison to a Spikformer [48] with equivalent parameters, our `AutoST` model delivers a performance boost of 1.32% while consuming merely 53.9% of the power. This experiment illustrates the flexibility and adaptability of our `AutoST` model, which is able to adapt to different resource constraints by tuning the balance between performance and efficiency.

## 5.4 Ablation Study

**Timestep Optimization.** Fig. 5a indicates a positive correlation between the number of timesteps and model performance. Although increasing timesteps usually improves accuracy, it simultaneously increases latency and energy consumption. A timestep count of 4 is found to significantly boost accuracy while maintaining efficiency, guiding our choice for further studies.

**Search Sample Efficiency.** As depicted in Fig. 5b and 5c, our evolutionary search method reveals that a configuration with 500 samples offers performance comparable to 1000 samples, but in half the search time. Therefore, we set the number of search samples to 500 in our study.

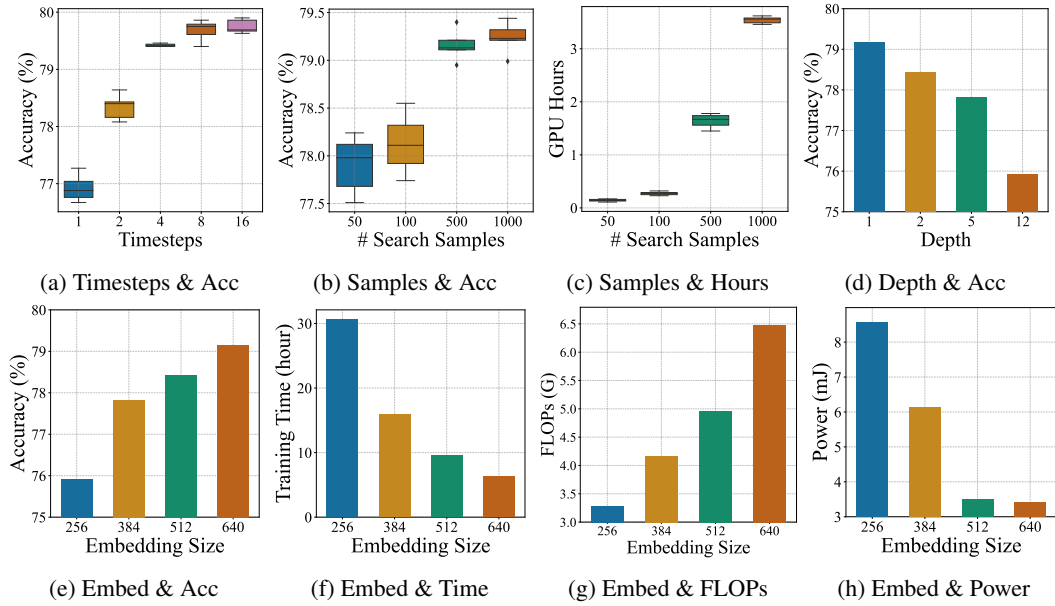


Figure 5: The ablation study of AutoST on the CIFAR-100 dataset. Subfigure (a) reveals that timesteps and accuracy exist a positive correlation. Subfigure (b-c) illustrates a trade-off between accuracy and search time. Subfigure (d-h) highlights the advantages of the search AutoST architectures: higher accuracy, lower training time, increased FLOPs, and decreased power consumption.

**Network Topology Analysis.** Our investigation into the search rule of AutoST reveals a predilection for shallower but wider network structures, a significant departure from conventional SNNs’ tendency for deeper, narrower configurations [45; 14]. We manually design and evaluate 4 different architectures with different embedding sizes and depths in the same parameter range to confirm this trend. As shown in Fig. 5d-5e, wider architectures consistently yield higher accuracy, which can be attributed to the specifics of SNNs. In specific, wider but shallow architecture can reduce quantization errors accumulated across layers [12; 6]. And this preference for wider Transformers is consistent with recent findings [42]. Furthermore, Fig. 5f indicates that wider architectures have a reduced training time. This is because shallower spiking layers mitigate the need for continual potential updates of spiking neurons during training, thereby significantly reducing training time.

**Effectiveness of AutoST metric.** We further delve into the FLOPs and power consumption of the aforementioned four architectures. As presented in Fig. 5g, a wider architecture exhibits higher FLOPs, attributable to its squared relationship with embedding size. Considering the superior performance of wider architectures, FLOPs can be utilized as a performance metric. Furthermore, since the FLOPs metric is independent of training dynamics, it can circumvent inherent SNN influences, thereby providing a reliable performance score. Moreover, Fig. 5g reveals a decrease in power with an increase in embedding size, reinforcing the use of AutoST as a promising approach for discovering Spiking Transformer architectures that are both high-performance and energy-efficient.

## 6 Conclusion and Future Work

In this paper, we introduce AutoST, a training-free NAS method for Spiking Transformers. Our framework can effectively discover high-performance and energy-efficient architectures with two innovative strategies. First, we propose a novel performance metric based on FLOPs, successfully addressing the inherent challenges of SNNs. Moreover, we leverage activation patterns to estimate energy consumption during initialization. Extensive experiments on both static and neuromorphic datasets have demonstrated AutoST’s adaptability and superior performance.

Nevertheless, directly implementing AutoST models on energy-constrained devices may result in substantial memory usage and power consumption. This observation paves the way for future research, particularly in the development of novel NAS techniques [7] that could mitigate these limitations. A promising direction includes the implementation of AutoST on specialized neuromorphic hardware. The low latency, energy efficiency, and minimal memory requirements of SNNs would be optimized by implementing AutoST on specialized neuromorphic hardware. This perspective direction makes AutoST an exciting prospect for both NAS and SNN research.

## References

- [1] Mohamed S. Abdelfattah, Abhinav Mehrotra, Lukasz Dudziak, and Nicholas D. Lane. Zero-cost proxies for lightweight nas. *arXiv preprint arXiv:2101.08134*, 2021.
- [2] Mohamed S. Abdelfattah, Abhinav Mehrotra, Lukasz Dudziak, and Nicholas D. Lane. Zero-cost proxies for lightweight nas. *arXiv preprint arXiv:2101.08134*, 2021.
- [3] Gabriel Bender, Pieter-Jan Kindermans, Barret Zoph, Vijay Vasudevan, and Quoc Le. Understanding and simplifying one-shot architecture search. In *International Conference on Machine Learning*, pages 550–559. PMLR, 2018.
- [4] Andrew Brock, Theodore Lim, James M. Ritchie, and Nick Weston. Smash: One-shot model architecture search through hypernetworks. *arXiv preprint arXiv:1708.05344*, 2017.
- [5] Tong Bu, Wei Fang, Jianhao Ding, PengLin Dai, Zhaofei Yu, and Tiejun Huang. Optimal ANN-SNN Conversion for High-accuracy and Ultra-low-latency Spiking Neural Networks. In *International Conference on Learning Representations*, 2021.
- [6] Tong Bu, Wei Fang, Jianhao Ding, PengLin Dai, Zhaofei Yu, and Tiejun Huang. Optimal ANN-SNN Conversion for High-accuracy and Ultra-low-latency Spiking Neural Networks. In *International Conference on Learning Representations*, 2021.
- [7] Han Cai, Chuang Gan, Tianzhe Wang, Zhekai Zhang, and Song Han. Once-for-all: Train one network and specialize it for efficient deployment. *arXiv preprint arXiv:1908.09791*, 2019.
- [8] Han Cai, Ligeng Zhu, and Song Han. Proxylessnas: Direct neural architecture search on target task and hardware. *arXiv preprint arXiv:1812.00332*, 2018.
- [9] Yongqiang Cao, Yang Chen, and Deepak Khosla. Spiking deep convolutional neural networks for energy-efficient object recognition. *International Journal of Computer Vision*, 113(1):54–66, 2015.
- [10] Wuyang Chen, Xinyu Gong, and Zhangyang Wang. Neural architecture search on imagenet in four gpu hours: A theoretically inspired perspective. *arXiv preprint arXiv:2102.11535*, 2021.
- [11] Shikuang Deng, Yuhang Li, Shanghang Zhang, and Shi Gu. Temporal Efficient Training of Spiking Neural Network via Gradient Re-weighting. *arXiv preprint arXiv:2202.11946*, 2022.
- [12] Jianhao Ding, Zhaofei Yu, Yonghong Tian, and Tiejun Huang. Optimal ann-snn conversion for fast and accurate inference in deep spiking neural networks. *arXiv preprint arXiv:2105.11654*, 2021.
- [13] Alexey Dosovitskiy, Lucas Beyer, Alexander Kolesnikov, Dirk Weissenborn, Xiaohua Zhai, Thomas Unterthiner, Mostafa Dehghani, Matthias Minderer, Georg Heigold, and Sylvain Gelly. An image is worth 16x16 words: Transformers for image recognition at scale. *arXiv preprint arXiv:2010.11929*, 2020.
- [14] Wei Fang, Zhaofei Yu, Yanqi Chen, Tiejun Huang, Timothée Masquelier, and Yonghong Tian. Deep residual learning in spiking neural networks. *Advances in Neural Information Processing Systems*, 34:21056–21069, 2021.
- [15] Wei Fang, Zhaofei Yu, Yanqi Chen, Timothée Masquelier, Tiejun Huang, and Yonghong Tian. Incorporating learnable membrane time constant to enhance learning of spiking neural networks. In *Proceedings of the IEEE/CVF International Conference on Computer Vision*, pages 2661–2671, 2021.
- [16] Bing Han, Gopalakrishnan Srinivasan, and Kaushik Roy. Rmp-snn: Residual membrane potential neuron for enabling deeper high-accuracy and low-latency spiking neural network. In *Proceedings of the IEEE/CVF Conference on Computer Vision and Pattern Recognition*, pages 13558–13567, 2020.
- [17] Minglun Han, Qingyu Wang, Tielin Zhang, Yi Wang, Duzhen Zhang, and Bo Xu. Complex dynamic neurons improved spiking transformer network for efficient automatic speech recognition. *arXiv preprint arXiv:2302.01194*, 2023.
- [18] Yifan Hu, Yujie Wu, Lei Deng, and Guoqi Li. Advancing residual learning towards powerful deep spiking neural networks. *arXiv preprint arXiv:2112.08954*, 2021.
- [19] Arthur Jacot, Franck Gabriel, and Clément Hongler. Neural tangent kernel: Convergence and generalization in neural networks. *Advances in neural information processing systems*, 31, 2018.
- [20] Youngeun Kim, Yuhang Li, Hyoungseob Park, Yeshwanth Venkatesha, and Priyadarshini Panda. Neural architecture search for spiking neural networks. In *Computer Vision–ECCV 2022: 17th European Conference, Tel Aviv, Israel, October 23–27, 2022, Proceedings, Part XXIV*, pages 36–56. Springer, 2022.

[21] Namhoon Lee, Thalaiyasingam Ajanthan, and Philip HS Torr. Snip: Single-shot network pruning based on connection sensitivity. *arXiv preprint arXiv:1810.02340*, 2018.

[22] Yuhang Li, Yufei Guo, Shanghang Zhang, Shikuang Deng, Yongqing Hai, and Shi Gu. Differentiable spike: Rethinking gradient-descent for training spiking neural networks. *Advances in Neural Information Processing Systems*, 34:23426–23439, 2021.

[23] Ming Lin, Pichao Wang, Zhenhong Sun, Hesen Chen, Xiuyu Sun, Qi Qian, Hao Li, and Rong Jin. Zen-nas: A zero-shot nas for high-performance image recognition. In *Proceedings of the IEEE/CVF International Conference on Computer Vision*, pages 347–356, 2021.

[24] Ze Liu, Yutong Lin, Yue Cao, Han Hu, Yixuan Wei, Zheng Zhang, Stephen Lin, and Baining Guo. Swin transformer: Hierarchical vision transformer using shifted windows. In *Proceedings of the IEEE/CVF International Conference on Computer Vision*, pages 10012–10022, 2021.

[25] Wolfgang Maass. Networks of spiking neurons: The third generation of neural network models. *Neural networks*, 10(9):1659–1671, 1997.

[26] Joe Mellor, Jack Turner, Amos Storkey, and Elliot J. Crowley. Neural architecture search without training. In *International Conference on Machine Learning*, pages 7588–7598. PMLR, 2021.

[27] Joe Mellor, Jack Turner, Amos Storkey, and Elliot J. Crowley. Neural architecture search without training. In *International Conference on Machine Learning*, pages 7588–7598. PMLR, 2021.

[28] Qingyan Meng, Mingqing Xiao, Shen Yan, Yisen Wang, Zhouchen Lin, and Zhi-Quan Luo. Training High-Performance Low-Latency Spiking Neural Networks by Differentiation on Spike Representation. In *Proceedings of the IEEE/CVF Conference on Computer Vision and Pattern Recognition*, pages 12444–12453, 2022.

[29] Shu Miao, Guang Chen, Xiangyu Ning, Yang Zi, Kejia Ren, Zhenshan Bing, and Alois Knoll. Neuromorphic vision datasets for pedestrian detection, action recognition, and fall detection. *Frontiers in neurorobotics*, 13:38, 2019.

[30] Etienne Mueller, Viktor Studenyak, Daniel Auge, and Alois Knoll. Spiking Transformer Networks: A Rate Coded Approach for Processing Sequential Data. In *2021 7th International Conference on Systems and Informatics (ICSAI)*, pages 1–5, November 2021.

[31] Byunggook Na, Jisoo Mok, Seongsik Park, Dongjin Lee, Hyeokjun Choe, and Sungroh Yoon. AutoSNN: Towards energy-efficient spiking neural networks. In *International Conference on Machine Learning*, pages 16253–16269. PMLR, 2022.

[32] Nitin Rathi and Kaushik Roy. DIET-SNN: Direct Input Encoding With Leakage and Threshold Optimization in Deep Spiking Neural Networks, December 2020.

[33] Esteban Real, Alok Aggarwal, Yanping Huang, and Quoc V. Le. Regularized evolution for image classifier architecture search. In *Proceedings of the Aaaai Conference on Artificial Intelligence*, volume 33, pages 4780–4789, 2019.

[34] Abhroneil Sengupta, Yuting Ye, Robert Wang, Chiao Liu, and Kaushik Roy. Going Deeper in Spiking Neural Networks: VGG and Residual Architectures. *Frontiers in Neuroscience*, 13, 2019.

[35] Hidenori Tanaka, Daniel Kunin, Daniel L. Yamins, and Surya Ganguli. Pruning neural networks without any data by iteratively conserving synaptic flow. *Advances in neural information processing systems*, 33:6377–6389, 2020.

[36] Ashish Vaswani, Noam Shazeer, Niki Parmar, Jakob Uszkoreit, Llion Jones, Aidan N. Gomez, Łukasz Kaiser, and Illia Polosukhin. Attention is all you need. *Advances in neural information processing systems*, 30, 2017.

[37] Chaoqi Wang, Guodong Zhang, and Roger Grosse. Picking winning tickets before training by preserving gradient flow. *arXiv preprint arXiv:2002.07376*, 2020.

[38] Ziqing Wang, Yuetong Fang, Jiahang Cao, Zhongrui Wang, and Renjing Xu. Efficient Spiking Transformer Enabled By Partial Information, October 2022.

[39] Yujie Wu, Lei Deng, Guoqi Li, Jun Zhu, and Luping Shi. Spatio-temporal backpropagation for training high-performance spiking neural networks. *Frontiers in neuroscience*, 12:331, 2018.

[40] Zhenzhi Wu, Hehui Zhang, Yihan Lin, Guoqi Li, Meng Wang, and Ye Tang. Liaf-net: Leaky integrate and analog fire network for lightweight and efficient spatiotemporal information processing. *IEEE Transactions on Neural Networks and Learning Systems*, 33(11):6249–6262, 2021.

[41] Man Yao, Guangshe Zhao, Hengyu Zhang, Yifan Hu, Lei Deng, Yonghong Tian, Bo Xu, and Guoqi Li. Attention spiking neural networks. *IEEE Transactions on Pattern Analysis and Machine Intelligence*, 2023.

[42] Xiaohua Zhai, Alexander Kolesnikov, Neil Houlsby, and Lucas Beyer. Scaling vision transformers. In *Proceedings of the IEEE/CVF Conference on Computer Vision and Pattern Recognition*, pages 12104–12113, 2022.

[43] Jiqing Zhang, Bo Dong, Haiwei Zhang, Jianchuan Ding, Felix Heide, Baocai Yin, and Xin Yang. Spiking Transformers for Event-Based Single Object Tracking. In *Proceedings of the IEEE/CVF Conference on Computer Vision and Pattern Recognition*, pages 8801–8810, 2022.

[44] Jiyuan Zhang, Lulu Tang, Zhaofei Yu, Jiwen Lu, and Tiejun Huang. Spike Transformer: Monocular Depth Estimation for Spiking Camera. In *Computer Vision–ECCV 2022: 17th European Conference, Tel Aviv, Israel, October 23–27, 2022, Proceedings, Part VII*, pages 34–52. Springer, 2022.

[45] Hanle Zheng, Yujie Wu, Lei Deng, Yifan Hu, and Guoqi Li. Going Deeper With Directly-Trained Larger Spiking Neural Networks, December 2020.

[46] Hanle Zheng, Yujie Wu, Lei Deng, Yifan Hu, and Guoqi Li. Going deeper with directly-trained larger spiking neural networks. In *Proceedings of the AAAI Conference on Artificial Intelligence*, volume 35, pages 11062–11070, 2021.

[47] Qinjin Zhou, Kekai Sheng, Xiawu Zheng, Ke Li, Xing Sun, Yonghong Tian, Jie Chen, and Rongrong Ji. Training-free transformer architecture search. In *Proceedings of the IEEE/CVF Conference on Computer Vision and Pattern Recognition*, pages 10894–10903, 2022.

[48] Zhaokun Zhou, Yuesheng Zhu, Chao He, Yaowei Wang, Shuicheng Yan, Yonghong Tian, and Li Yuan. Spikformer: When Spiking Neural Network Meets Transformer. *arXiv preprint arXiv:2209.15425*, 2022.

[49] Barret Zoph and Quoc V. Le. Neural architecture search with reinforcement learning. *arXiv preprint arXiv:1611.01578*, 2016.

[50] Barret Zoph, Vijay Vasudevan, Jonathon Shlens, and Quoc V. Le. Learning transferable architectures for scalable image recognition. In *Proceedings of the IEEE Conference on Computer Vision and Pattern Recognition*, pages 8697–8710, 2018.